

# On the Sr I $\lambda 4607$ Å Hanle depolarization signals in the quiet Sun

J. Sánchez Almeida

Instituto de Astrofísica de Canarias, 38205 La Laguna, Tenerife, Spain  
e-mail: jos@iac.es

Received 19 November 2004 / Accepted 23 March 2005

**Abstract.** The Hanle depolarization signals of Sr I  $\lambda 4607$  Å have been used to estimate the unsigned magnetic flux and magnetic energy existing in the quiet Sun photosphere. However, the Sr I  $\lambda 4607$  Å Hanle signals are not sensitive to the unsigned flux and energy. They only bear information on the fraction of photosphere occupied by magnetic field strengths smaller than the Hanle saturation, which do not contribute to the unsigned flux and energy. We deduce an approximate expression for the relationship between magnetic fill factor and Hanle signal. When applied to existing Hanle depolarization measurements, it indicates that only 40% of the quiet Sun is filled by magnetic fields with a strength smaller than 60 G. The remaining 60% of the surface has field strengths above this limit. Such constraint will be needed to determine the distribution of magnetic field strengths existing in the quiet Sun.

**Key words.** polarization – Sun: magnetic fields – Sun: photosphere

## 1. Introduction

Most of the solar surface does not show significant polarization signals in traditional magnetic field measurements. However, the magnetism of this so-called quiet Sun appears when the polarimetric sensitivity and the angular resolution exceed a threshold (e.g., Sánchez Almeida 2004, and references therein). Magnetic fields in the quiet Sun were discovered in the seventies by Livingston & Harvey (1975) and Smithson (1975), but they experience a revival of interest due to the significant amounts of magnetic flux and energy that the quiet Sun may store (Stenflo 1982; Zirin 1987; Yi et al. 1993; Sánchez Almeida 1998).

The quiet Sun magnetic fields<sup>1</sup> have inspired theoretical studies on their origin (Petrovay & Szakaly 1993; Cattaneo 1999) and interplay with granular convection (Cattaneo et al. 2001; Stein & Nordlund 2002; Vögler & Schüssler 2003), as well as on the coupling with coronal magnetic structures (Schrijver & Title 2003; Goodman 2004). Unfortunately, we still lack a firm theoretical framework to describe their nature. From an observational point of view, our understanding has also improved including the complex magnetic topology of these magnetic fields (Sánchez Almeida et al. 1996; Sigwarth et al. 1999; Sánchez Almeida & Lites 2000; Lites 2002; Sánchez Almeida et al. 2003b), the existence large amounts of unsigned magnetic flux and energy (Sánchez Almeida & Lites 2000; Domínguez Cerdeña et al. 2003), the variety of intrinsic field strengths (Faurobert-Scholl et al. 1995; Bianda et al. 1999; Lin & Rimmele 1999; Sánchez Almeida & Lites 2000; Socas-Navarro & Sánchez Almeida 2002), and some

other properties (see Sánchez Almeida 2004). All these advances notwithstanding, the observational characterization of the quiet Sun fields is unsatisfactory. The complex topology of the fields makes all present measurements prone to severe bias, a fact that must be acknowledged and resolved before developing a reliable observational picture of quiet Sun magnetism.

Due to the complexity of the fields, they have to be characterized in terms of probability density functions (PDFs). The magnetic field strength PDF is particularly useful. It gives the fraction of the solar photosphere occupied by magnetic fields with a given field strength. The two first moments of this PDF provide the unsigned magnetic flux density and the magnetic energy density, respectively (e.g. Sánchez Almeida 2004). From an observational point of view, the PDF has to be assembled from various different measurements. The polarization signals created by Zeeman effect are most sensitive to magnetic field strengths larger than a few hundred G. The Hanle effect induced signals respond to field strengths below this limit.

A significant part of what we know about the weakest fields comes from the interpretation of the Hanle depolarization signals of Sr I  $\lambda 4607$  Å (Stenflo 1982; Faurobert-Scholl 1993; Faurobert-Scholl et al. 1995; Stenflo et al. 1997; Faurobert et al. 2001). In particular, it has been shown that the observed Hanle depolarization signals of Sr I  $\lambda 4607$  Å require an average field of 130 G and a magnetic energy density of  $1.3 \times 10^3$  erg cm<sup>-3</sup> (Trujillo Bueno et al. 2004). However, this mean field exceeds the limit able to induce a significant Hanle depolarization signal in this line ( $\sim 100$  G; see, Sect. 2.1; or Faurobert et al. 2001). As we will discuss (Sect. 3), this seeming inconsistency results from an assumption which turns out to be decisive in assigning a mean field and a magnetic energy to the observed Hanle depolarization signals, namely, the shape of the PDF. Such

<sup>1</sup> Often referred to as Inter-Network fields, Intra-Network fields or simply IN fields.

PDF-dependence of the inference casts doubts on the results and, more importantly, it urges us to understand what is the true information provided by Sr I  $\lambda 4607$  Å. Using a simplified (yet realistic) treatment of the radiative transfer, we explore the diagnostic content under the conditions to be expected in the quiet solar photosphere, with a mean field strength larger than the saturation field of the Hanle effect. We find that the Hanle signals only depend on to the fill factor of magnetic fields below the Hanle saturation. They provide almost no constraint on the mean field strength and magnetic energy that may exist in the quiet Sun. This fact has to be taken into account when using information from Sr I  $\lambda 4607$  Å to determine the PDF of the quiet Sun magnetic field strength.

The work is organized as follows: Sect. 2.1 lists the approximations used to carry out the Hanle depolarization syntheses. The degree of realism of this treatment is discussed in Sect. 2.2. The Hanle signals to be expected from an exponential PDF with a mean field of 130 G are analyzed in detail in Sect. 3. The actual diagnostic content of the Sr I  $\lambda 4607$  Å Hanle signals is worked out in Sect. 4. An example of a PDF with unbound magnetic flux and energy compatible with the observed Hanle signals is shown in Sect. 5. Finally, the ways in which these results constrain the distribution of magnetic fields existing in the quiet Sun are discussed in Sect. 6.

## 2. Hanle depolarization of Sr I $\lambda 4607$ Å

### 2.1. Basic properties and notation

The Hanle depolarization of Sr I  $\lambda 4607$  Å can be expressed as

$$Q/Q_0 \simeq W_B(B) = 1 - \frac{2}{5} \left( \frac{\gamma_H^2}{1 + \gamma_H^2} + \frac{4\gamma_H^2}{1 + 4\gamma_H^2} \right), \quad (1)$$

where  $Q/Q_0$  is the ratio between the observed linear polarization  $Q$  and the polarization if there were no magnetic field  $Q_0$ . The symbol  $\gamma_H$  parameterizes the magnetic field of the micro-turbulent distribution of magnetic fields with random orientation and constant field strength  $B$ ,

$$\gamma_H = B/B_H. \quad (2)$$

The so-called Hanle parameter  $B_H$  scales linearly with the radiative transition rate plus the depolarizing collision rate, and it can be computed from the temperature and density according to the prescription in Faurobert et al. (2001, Sect. 3). The relationship (1) is an approximation that holds when the Hanle depolarization results from a single scattering (Stenflo 1982; Landi Degl'Innocenti 1985; Faurobert et al. 2001). It is a good approximation for this particular line in the quiet Sun (see Sect. 2.2, below). The depolarization  $W_B(B)$  does not vary significantly with  $B$  when  $B \gg B_H$ . This property is often referred to as the saturation of the Hanle signal, implying that the Hanle depolarization is not sensitive to fields much larger than  $B_H$ . Figure 1a shows  $W_B(B)$  when  $B_H = 47$  G. Note that the depolarization barely changes for  $B > 100$  G or  $2B_H$ . The value for  $B_H$  used above is typical of Sr I  $\lambda 4607$  Å in the photospheric heights where the line is formed, say, from 200 km

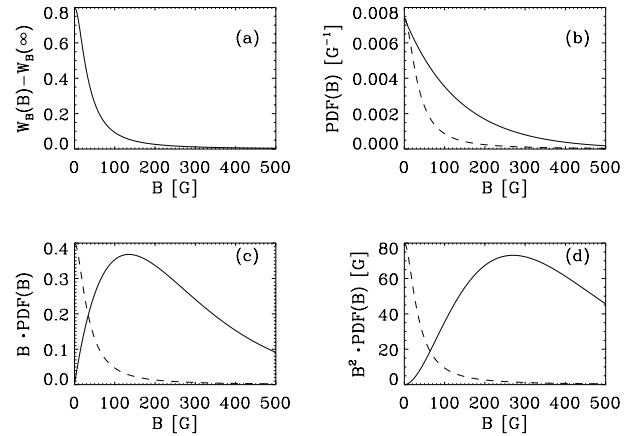


**Fig. 1.** a) Sr I  $\lambda 4607$  Å Hanle depolarization signals versus magnetic field strength for  $B_H$  typical of the upper photosphere of the quiet Sun. The depolarization signals have no significant contribution when  $B$  is, say, larger than 100 G. b) Exponential PDF with mean 130 G (the solid line). c) Unsigned flux density per unit of magnetic field strength for the PDF shown in b). d) Magnetic energy density per unit of magnetic field strength. The dashed lines in b–d) represent  $[W_B(B) - W_B(\infty)]$  scaled to fit in the plots.

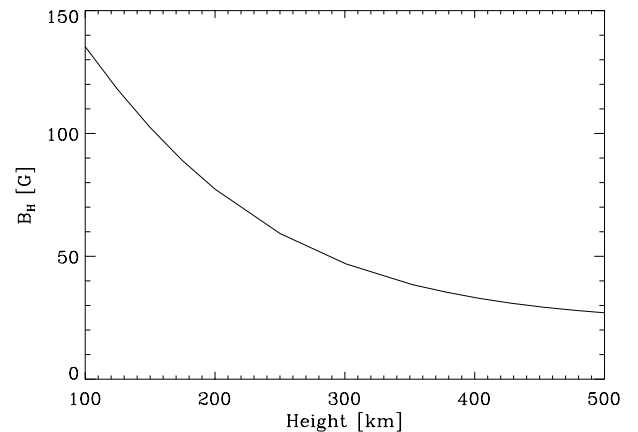


**Fig. 2.**  $B_H$  as a function of height in the atmosphere for the quiet Sun model atmosphere by Maltby et al. (1986). Note that  $B_H$  is smaller than 50 G above 250 km, where Sr I  $\lambda 4607$  Å is formed.

to 400 km above the base of the photosphere (Faurobert-Scholl et al. 1995, which also show how the range of heights contributing to Hanle signals does not depend very much on the heliocentric angle). Figure 2 shows  $B_H$  as a function of height in a quiet Sun model atmosphere (Maltby et al. 1986).  $B_H$  is of the order of 77 G at 200 km and 33 G at 400 km, with a value of 47 G in the middle of the range. In the case that the magnetic field strength is not unique but has a distribution of values according to a PDF  $P(B)$ , then the depolarization signal  $\langle Q/Q_0 \rangle$  equals the average depolarization factor (see Landi Degl'Innocenti 1985, Sect. 3),

$$\langle Q/Q_0 \rangle \simeq \int_0^\infty P(B)W_B(B)dB. \quad (3)$$

Since  $\langle Q/Q_0 \rangle \neq 0$  when  $B \rightarrow \infty$ , the actual range of polarization signals sensitive to magnetic field strength variations is only a part of  $\langle Q/Q_0 \rangle$ , namely,

$$\langle Q/Q_0 \rangle - \langle Q_\infty/Q_0 \rangle = \int_0^\infty P(B)[W_B(B) - W_B(\infty)]dB, \quad (4)$$

where  $Q_\infty$  is the linear polarization signal to be expected if only fields larger than the Hanle saturation are present in the atmosphere. For these PDFs,  $P(B) \neq 0$  only when  $W_B(B) \approx W_B(\infty)$ , so that

$$\langle Q_\infty/Q_0 \rangle \approx \int_0^\infty P(B)W_B(\infty)dB = W_B(\infty) = 1/5. \quad (5)$$

Two particular cases are of special interest. They have been used to assign unsigned magnetic fluxes and magnetic energies to observed Sr I  $\lambda 4607$  Å Hanle signals. In the case that  $P(B)$  is a very narrow function of  $B$ , namely,

$$P(B) \neq 0 \text{ only when } |B - \widehat{B}| < \Delta B \ll B_H, \quad (6)$$

then

$$\begin{aligned} \langle (Q - Q_\infty)/Q_0 \rangle &\approx \int_0^\infty P(B)[W_B(\widehat{B}) - W_B(\infty)]dB \\ &\approx W_B(\widehat{B}) - W_B(\infty). \end{aligned} \quad (7)$$

The second case assumes  $P(B)$  to be an exponential function of mean  $B_0$ ,

$$P(B) = B_0^{-1} \exp(-B/B_0). \quad (8)$$

Then Eq. (4) admits a compact expression,

$$\langle (Q - Q_\infty)/Q_0 \rangle = \frac{2}{5} \left[ \frac{B_H}{B_0} f\left(\frac{B_H}{B_0}\right) + \frac{B_H}{2B_0} f\left(\frac{B_H}{2B_0}\right) \right], \quad (9)$$

with

$$f(x) = \int_0^\infty \frac{\exp(-xy)}{1+y^2} dy. \quad (10)$$

## 2.2. Accuracy of the single scattering approximation

The equations described in the previous section hold for a single scattering event. However, they are also a good representation of the Sr I  $\lambda 4607$  Å Hanle signal when a more complete treatment of the radiative transfer is considered. Faurobert et al. (2001) compare full 1D NLTE syntheses with Eq. (7), and they conclude that both approaches lead to the same  $\widehat{B}$  within the error bars of the observations. Trujillo Bueno et al. (2004) calculate the Sr I  $\lambda 4607$  Å Hanle depolarization in a realistic 3D hydrodynamic simulation, considering a 15 level Sr I atom and solving the NLTE problem in three dimensions. Equations (7) and (9) still provide magnetic fields in close agreement with the full calculation. The depolarization signal found by Trujillo Bueno et al. (2004) is

$$\langle Q/Q_0 \rangle \approx 0.41 \pm 0.04, \quad (11)$$

for  $0.2 \leq \mu \leq 0.6$  ( $\mu$  stands for the cosine of the heliocentric angle). In order to reproduce these observations, Trujillo Bueno et al. (2004) need an exponential PDF with

$B_0 = 130$  G or, alternatively, a delta-function PDF with  $\widehat{B} = 60$  G. These values of  $B_0$  and  $\widehat{B}$  also reproduce the observable (11) under the single scattering approximation. Using  $B_H = 47$  G (which is the mean value in the atmospheric layers where the Sr I  $\lambda 4607$  Å Hanle depolarization is formed), Eq. (9) with  $B_0 = 130$  G leads to

$$\langle Q/Q_0 \rangle \approx 0.42. \quad (12)$$

In addition, one obtains exactly the same depolarization setting  $\widehat{B} = 57$  G in Eq. (7).

The large differences between the mean field strengths deduced by Faurobert et al. (2001,  $\widehat{B} \approx 25$  G) and Trujillo Bueno et al. (2004,  $\widehat{B} \approx 60$  G) are not due the different ways in which they synthesize the Hanle depolarization  $\langle Q/Q_0 \rangle$  in terms of a turbulent magnetic field. This step of the estimate seems to be independent of the details of the modeling, and it is properly described by Eq. (3). The differences are due to the estimate of the scattering signals to be expected for no magnetic field (i.e., the quantity  $\langle Q_0 \rangle$ ). Although they start from similar observed  $\langle Q \rangle$ , Faurobert et al. (2001) infer  $\langle Q/Q_0 \rangle \approx 0.6$  instead of the depolarization in Eq. (11). If Trujillo Bueno et al. (2004) would have found  $\langle Q/Q_0 \rangle = 0.6$ , their treatment would have assigned  $\widehat{B} \approx 30$  G to this signal. Such a conclusion can be readily inferred from their Fig. 1 by artificially increasing the observed  $\langle Q \rangle$  to yield  $\langle Q/Q_0 \rangle \approx 0.6$ . (See also Shchukina & Trujillo Bueno 2003.)

## 3. Largest field strength contributing to the Hanle signals

This section analyzes in detail the case of an exponential PDF with  $B_0 = 130$ . It illustrates the difficulties in inferring unsigned magnetic fluxes and energies from the quiet Sun Hanle depolarization signals of Sr I  $\lambda 4607$  Å.

Let us define  $B_{\max}$  as the largest field strength that produces a significant contribution to the observed signal. The contribution would be regarded as significant only if it is above the observational error  $\epsilon$ . Then  $B_{\max}$  is defined as

$$\epsilon = \frac{\int_{B_{\max}}^\infty P(B)[W_B(B) - W_B(\infty)]dB}{\int_0^\infty P(B)[W_B(B) - W_B(\infty)]dB}, \quad (13)$$

which follows from Eq. (4) and the condition that all magnetic fields with  $B > B_{\max}$  change the depolarization by less than a factor  $\epsilon$ . Figure 3, the solid line, shows  $\epsilon = \epsilon(B_{\max})$  when  $B_H = 47$  G and  $B_0 = 130$  G, i.e., the parameters that characterize the observed depolarization. The true observational error is larger than 10% (see Sect. 2.2). Note that  $\epsilon < 0.1$  when  $B_{\max} \geq 100$  G, meaning that those magnetic fields of the exponential PDF with  $B > 100$  G do not contribute to the observed signal.

The unsigned magnetic flux density and magnetic energy density can be computed from the first two moments of the PDF (e.g. Sánchez Almeida 2004). However, the magnetic fields that determine the first two moments of an exponential PDF with

<sup>2</sup> The estimate by Trujillo Bueno et al. (2004) is to be favored for quiet Sun diagnosis since it is based on realistic MHD simulations, 3D scattering polarization calculations, and a complex Sr atom.

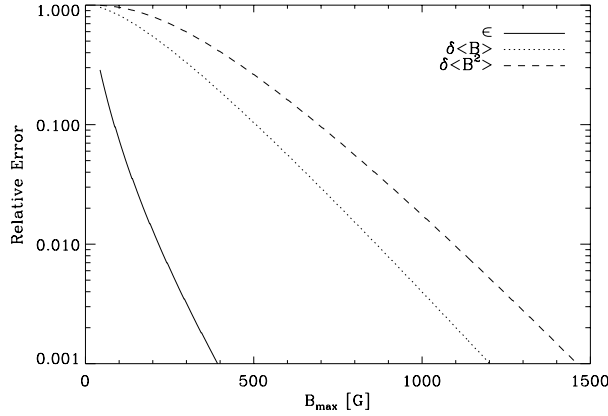


**Fig. 3.** Relative errors of the Hanle depolarization signals produced by neglecting all magnetic fields larger  $B_{\max}$  (the solid line). It is smaller than the 10% observational error when  $B_{\max} > 87$  G. Relative contribution to the unsigned magnetic flux density (the dotted line) and the magnetic energy density (the dashed line) produced by magnetic fields larger than  $B_{\max}$ .

$B_0 = 130$  G exceed  $B_{\max} \approx 100$  G. Consequently, the unsigned flux and the energy assigned assuming an exponential PDF are not constrained by the observations. The first two moments are given by

$$\langle B \rangle = \int_0^{\infty} B \cdot P(B) dB, \quad (14)$$

and

$$\langle B^2 \rangle = \int_0^{\infty} B^2 \cdot P(B) dB. \quad (15)$$

The integrands of Eqs. (14) and (15) describe the contribution of each field strength to the two moments, and they are shown in Figs. 1c and 1d. The figures include a scaled version of  $[W_B(B) - W_B(\infty)]$  (the dashed lines), which indicates the range of field strengths constrained by the observations. Obviously, most of the unsigned flux (related to the first moment) and energy density (second moment) are provided by field strengths larger than 100 G. It is possible to quantify the bias defining the fraction of unsigned flux density made up by considering field strengths which do not contribute to the Hanle signals, explicitly,

$$\delta \langle B \rangle = \frac{\int_{B_{\max}}^{\infty} B \cdot P(B) dB}{\int_0^{\infty} B \cdot P(B) dB}. \quad (16)$$

Similarly, the fraction of energy density that comes from the tail of the PDF, and so, does not contribute to the Hanle signals, is

$$\delta \langle B^2 \rangle = \frac{\int_{B_{\max}}^{\infty} B^2 \cdot P(B) dB}{\int_0^{\infty} B^2 \cdot P(B) dB}. \quad (17)$$

Both  $\delta \langle B \rangle$  and  $\delta \langle B^2 \rangle$  are shown in Fig. 3. It turns out that 90% of the Hanle signals ( $\epsilon = 0.1$ ) are produced by  $B < 86$  G. The tail of magnetic fields that do not contribute to the Hanle signals actually produce 86% of  $\langle B \rangle$  and 97% of  $\langle B^2 \rangle$ . In other words, the result by Trujillo Bueno et al. (2004) that

$\langle B \rangle = B_0 = 130$  G and  $\langle B^2 \rangle / (8\pi) = (2B_0^2) / (8\pi) = 1.3 \times 10^3$  erg cm $^{-3}$  is based on the assumption of the shape of the PDF, but it is not constrained by the observations. By changing the tail of large field strengths of the PDF one can modify in an arbitrary manner the unsigned flux and energy, but still producing the observed Hanle depolarization. An example is given in Sect. 5.

#### 4. What does the Hanle depolarization of Sr I $\lambda 4607$ Å diagnose?

Let us consider PDFs with the properties to be expected for the solar quiet Sun magnetic fields. The Hanle signals are produced by magnetic fields within the bandpass where  $[W_B(B) - W_B(\infty)] \neq 0$ , which is of the order of  $2B_H$ . Then the Hanle signals can be estimated as

$$\langle (Q - Q_{\infty}) / Q_0 \rangle \approx \int_0^{2B_H} P(B) [W_B(B) - W_B(\infty)] dB. \quad (18)$$

In addition, the quiet Sun PDF should spread out over a range of field strengths larger than  $B_H$  (see, e.g., Sánchez Almeida 2004), so that within the bandpass of interest, it can be approximated by a linear expansion,

$$P(B) \approx a + b(B - B'). \quad (19)$$

Obviously,

$$a = \frac{1}{2B'} \int_0^{2B'} P(B) dB. \quad (20)$$

If one chooses  $B'$  to be

$$B' = \frac{\int_0^{2B_H} B [W_B(B) - W_B(\infty)] dB}{\int_0^{2B_H} [W_B(B) - W_B(\infty)] dB}, \quad (21)$$

then the Hanle depolarization signals given by Eq. (18) are independent of the slope  $b$ ,

$$\langle (Q - Q_{\infty}) / Q_0 \rangle = C \int_0^{2B'} P(B) dB, \quad (22)$$

$$C = \frac{1}{2B'} \int_0^{2B_H} [W_B(B) - W_B(\infty)] dB.$$

The integrals defining  $B'$  and  $C$  can be solved analytically to render

$$B' \approx 0.65 B_H, \quad C \approx 0.54, \quad (23)$$

and, consequently,

$$\langle (Q - Q_{\infty}) / Q_0 \rangle \approx 0.54 \int_0^{1.3B_H} P(B) dB. \quad (24)$$

The Hanle depolarization signals scale with the fill factor of fields with strength smaller than  $1.3B_H$ . As expected, the Hanle depolarization of Sr I  $\lambda 4607$  Å is independent of the actual unsigned magnetic flux or magnetic energy of the distribution.

The approximate Eq. (24) has been tested for the case where  $P(B)$  is exponential. Figure 4a shows the variation of the

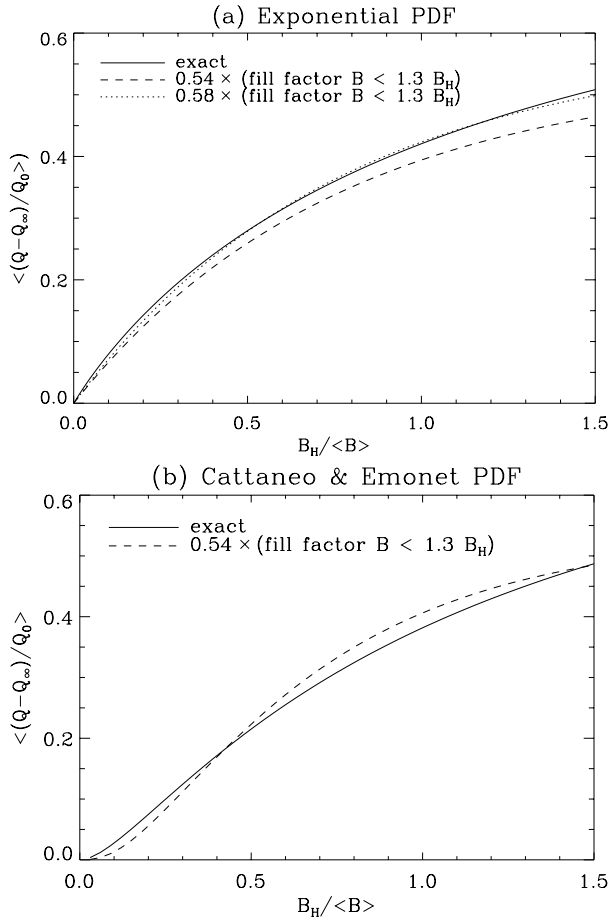


**Fig. 4.** **a)** Hanle depolarization as a function of  $B_H/\langle B \rangle$  when the PDF is an exponential function (the solid line). It is approximately given by half the fill factor of magnetic fields smaller than  $1.3B_H$  (the dashed line). **b)** Hanle depolarization as a function of  $B_H/\langle B \rangle$  for the PDF of the turbulent dynamo simulations by Emonet & Cattaneo (2001), as described by Sánchez Almeida et al. (2003a) (the solid line). The approximate relationship worked out in the paper also provides a fair representation of the Hanle signals.

Hanle depolarization signals with  $B_H/\langle B \rangle$ , where  $\langle B \rangle$  stands for the mean magnetic field of the distribution. The solid line has been computed from the exact solution (9), whereas the dashed line follows from the approximate Eq. (24). The agreement is good, and it improves to excellent if  $C = 0.58$  (the dotted line). Figure 4b also shows the exact and the approximate Hanle signals deduced for the numerical turbulent dynamo PDF used in Sánchez Almeida et al. (2003a). The agreement of the approximation is also satisfactory. Despite the simplistic approximation leading to the relationship (24), it reproduces within 10% the exact relationship (4). The agreement is expected independently of the (unknown) details of the quiet Sun PDF, since Eq. (24) is based on very general assumptions.

Equation (24) satisfies the observation (11) when magnetic field strengths smaller than 60 G occupy 40% of the quiet Sun. Obviously, the exponential PDF chosen by Trujillo Bueno et al. (2004) fulfills this criterion. The turbulent dynamo PDF used by Sánchez Almeida et al. (2003a, Sect. 5) does so too.

## 5. Example of unbound magnetic flux and energy compatible with the observed Hanle signals

From the arguments above, it is clear that the unsigned magnetic flux and energy of the distribution are not related to the Hanle signals. This section shows an example reinforcing the point. We show a PDF producing the observed polarization with an arbitrarily large magnetic flux and energy. Consider the combination of exponentials,

$$P(B) = \beta B_1^{-1} \exp(-B/B_1) + (1 - \beta) B_2^{-1} \exp(-B/B_2), \quad (25)$$

with  $B_1 \ll B_H \ll B_2$ . The second exponential does not contribute to the Hanle depolarization signals, since it is given by Eq. (9) with  $B_H/B_0 \rightarrow 0$ . On the other hand,  $f(x) \rightarrow x^{-1}$  when  $x \rightarrow \infty$ , which together with Eqs. (9) and (5) lead to

$$\langle Q/Q_0 \rangle \simeq (1 + 4\beta)/5. \quad (26)$$

The value  $\beta \simeq 0.27$  satisfies the observed depolarization (11). On the other hand, the two moments (14) and (15) only depend on the second component,

$$\langle B \rangle = \beta B_1 + (1 - \beta) B_2 \simeq (1 - \beta) B_2, \quad (27)$$

$$\langle B^2 \rangle = 2\beta B_1^2 + 2(1 - \beta) B_2^2 \simeq 2(1 - \beta) B_2^2. \quad (28)$$

since  $B_1 \ll B_2$ . Then the unsigned flux and the energy corresponding to Eq. (25) can be arbitrarily large by increasing  $B_2$  with no modification of the Hanle signal (Eq. (26)).

## 6. Conclusions

The Hanle depolarization signals of Sr I  $\lambda 4607$  Å are insensitive to the magnetic flux and magnetic energy existing in the quiet Sun photosphere. They only bear information on the fraction of surface occupied by magnetic field strengths smaller than some  $2B_H$ , equivalent to 100 G when the so-called Hanle parameter  $B_H$  is 50 G. In order to gain physical insight into the diagnostic provided by the Sr I  $\lambda 4607$  Å Hanle depolarization signals, we estimate the signals to be expected when the magnetic atmosphere contains disorganized magnetic fields with field strengths from zero to a value exceeding  $B_H$ . The expected signal is given by Eq. (24). It is a fixed fraction (54%) of the fill factor of magnetic fields whose strengths are smaller than  $1.3B_H$ .

Our result implies that the findings by Trujillo Bueno et al. (2004) should be updated, in particular, the Hanle depolarization signals that they provide (Eq. (12)) do not imply an unsigned flux and a magnetic energy density. They imply that 40% of the quiet Sun is covered by fields whose strength is smaller than 60 G. In other words, some 60% of the quiet Sun has field strengths larger than 60 G. Obviously, this result is consistent with a distribution of magnetic fields having a magnetic flux and energy even larger than those inferred by Trujillo Bueno et al. (2004), but the unsigned flux and energy are not constrained by the Hanle signals. The magnetic flux and energy are constrained by the polarization signals induced via the Zeeman effect, which contain information on the hG and kG field strengths of the quiet Sun PDF (see

Sánchez Almeida & Lites 2000). For example, the magnetic energy density of the kG fields observed by Domínguez Cerdeña et al. (2003), which occupy only 2% of the surface, actually contain as much energy as an exponential PDF with  $B_0 = 130$  G.

We lack a reliable quiet Sun PDF to represent the whole range of observed field strengths from zero to two kG. This PDF would have to be assembled piecing together information from various sources, as indicated in Sánchez Almeida (2004). The results of our analysis are needed to complete such observational work, since they clarify how the Sr I  $\lambda$ 4607 Å Hanle signals constrain the empirical PDF.

*Acknowledgements.* The work has partly been funded by the Spanish Ministry of Science and Technology, project AYA2004-05792, as well as by the EC contract HPRN-CT-2002-00313.

## References

- Bianda, M., Stenflo, J. O., & Solanki, S. K. 1999, A&A, 350, 1060  
 Cattaneo, F. 1999, ApJ, 515, L39  
 Cattaneo, F., Lenz, D., & Weiss, N. O. 2001, ApJ, 563, L91  
 Domínguez Cerdeña, I., Kneer, F., & Sánchez Almeida, J. 2003, ApJ, 582, L55  
 Emonet, T., & Cattaneo, F. 2001, ApJ, 560, L197  
 Faurobert, M., Arnaud, J., Vigneau, J., & Frish, H. 2001, A&A, 378, 627  
 Faurobert-Scholl, M. 1993, A&A, 268, 765  
 Faurobert-Scholl, M., Feautrier, N., Machefer, F., Petrovay, K., & Spielfiedel, A. 1995, A&A, 298, 289  
 Goodman, M. L. 2004, A&A, 424, 691  
 Landi Degl'Innocenti, E. 1985, Sol. Phys., 102, 1  
 Lin, H., & Rimmele, T. 1999, ApJ, 514, 448  
 Lites, B. W. 2002, ApJ, 573, 431  
 Livingston, W. C., & Harvey, J. W. 1975, BAAS, 7, 346  
 Maltby, P., Avrett, E. H., Carlsson, M., et al. 1986, ApJ, 306, 284  
 Petrovay, K., & Szakaly, G. 1993, A&A, 274, 543  
 Sánchez Almeida, J. 1998, in Three-Dimensional Structure of Solar Active Regions, ed. C. E. Alissandrakis, & B. Schmieder (San Francisco: ASP), ASP Conf. Ser., 155, 54  
 Sánchez Almeida, J., Landi Degl'Innocenti, E., Martínez Pillet, V., & Lites, B. W. 1996, ApJ, 466, 537  
 Sánchez Almeida, J., & Lites, B. W. 2000, ApJ, 532, 1215  
 Sánchez Almeida, J. 2004, in The Solar-B Mission and the Forefront of Solar Physics, ed. T. Sakurai, & T. Sekii (San Francisco: ASP), ASP Conf. Ser., 325, 115 [arXiv:astro-ph/0404053]  
 Sánchez Almeida, J., Emonet, T., & Cattaneo, F. 2003a, ApJ, 585, 536  
 Sánchez Almeida, J., Domínguez Cerdeña, I., & Kneer, F. 2003b, ApJ, 597, L177  
 Schrijver, C. J., & Title, A. M. 2003, ApJ, 597, L165  
 Shchukina, N. G., & Trujillo Bueno, J. 2003, in Solar Polarization Workshop 3, ed. J. Trujillo-Bueno & J. Sánchez Almeida (San Francisco: ASP), ASP Conf. Ser., 307, 336  
 Sigwarth, M., Balasubramaniam, K. S., Knölker, M., & Schmidt, W. 1999, A&A, 349, 941  
 Smithson, R. C. 1975, BAAS, 7, 346  
 Socas-Navarro, H., & Sánchez Almeida, J. 2002, ApJ, 565, 1323  
 Stein, R. F., & Nordlund, Å. 2002, in IAU Coll., 188, ed. H. Sawaya-Lacoste, ESA SP-505 (Noordwijk: ESA Publications Division), 83  
 Stenflo, J. O. 1982, Sol. Phys., 80, 209  
 Stenflo, J. O., Bianda, M., Keller, C. U., & Solanki, S. K. 1997, A&A, 322, 985  
 Trujillo Bueno, J., Shchukina, N. G., & Asensio Ramos, A. 2004, Nature, 430, 326  
 Vögler, A., & Schüssler, M. 2003, Astron. Nachr., 324, 399  
 Yi, Z., Jensen, E., & Engvold, O. 1993, in The Magnetic and Velocity Fields of Solar Active Regions, ed. H. Zirin, G. Ai, & H. Wang, San Francisco, ASP Conf. Ser., 46, 232  
 Zirin, H. 1987, Sol. Phys., 110, 101